School of Natural Sciences and Mathematics

Amplitude Analysis of the Decays $\eta' \rightarrow \pi^+\pi^-\pi^0$ and $\eta' \rightarrow \pi^0\pi^0\pi^0$

UT Dallas Author(s):

Xinchou Lou

Amplitude Analysis of the Decays $\eta' \to \pi^+\pi^-\pi^0$ and $\eta' \to \pi^0\pi^0\pi^0$

M. Ablikim,[1] M. N. Achasov,[9,e] X. C. Ai,[1] O. Albayrak,[5] M. Albrecht,[4] D. J. Ambrose,[44] A. Amoroso,[49a,49c] F. F. An,[1] Q. An,[46,a] J. Z. Bai,[1] R. Baldini Ferroli,[20a] Y. Ban,[31] D. W. Bennett,[19] J. V. Bennett,[5] M. Bertani,[20a] D. Bettoni,[21a] J. M. Bian,[43] F. Bianchi,[49a,49c] E. Boger,[23,c] I. Boyko,[23] R. A. Briere,[5] H. Cai,[51] X. Cai,[1,a] O. Cakir,[40a] A. Calcaterra,[20a] G. F. Cao,[1] S. A. Cetin,[40b] J. F. Chang,[1,a] G. Chelkov,[23,c,d] G. Chen,[1] H. S. Chen,[1] H. Y. Chen,[2] J. C. Chen,[1] M. L. Chen,[1,a] S. Chen,[41] S. J. Chen,[29] X. Chen,[1,a] X. R. Chen,[26] Y. B. Chen,[1,a] H. P. Cheng,[17] X. K. Chu,[31] G. Cibinetto,[21a] H. L. Dai,[1,a] J. P. Dai,[34] A. Dbeyssi,[14] D. Dedovich,[23] Z. Y. Deng,[1] A. Denig,[22] I. Denysenko,[23] M. Destefanis,[49a,49c] F. De Mori,[49a,49c] Y. Ding,[27] C. Dong,[30] J. Dong,[1,a] L. Y. Dong,[1] M. Y. Dong,[1,a] Z. L. Dou,[29] S. X. Du,[53] P. F. Duan,[1] J. Z. Fan,[39] J. Fang,[1,a] S. S. Fang,[1] X. Fang,[46,a] Y. Fang,[1] R. Farinelli,[21a,21b] L. Fava,[49b,49c] O. Fedorov,[23] F. Feldbauer,[22] G. Felici,[20a] C. Q. Feng,[46,a] E. Fioravanti,[21a] M. Fritsch,[14,22] C. D. Fu,[1] Q. Gao,[1] X. L. Gao,[46,a] X. Y. Gao,[2] Y. Gao,[39] Z. Gao,[46,a] I. Garzia,[21a] K. Goetzen,[10] L. Gong,[30] W. X. Gong,[1,a] W. Gradl,[22] M. Greco,[49a,49c] M. H. Gu,[1,a] Y. T. Gu,[12] Y. H. Guan,[1] A. Q. Guo,[1] L. B. Guo,[28] R. P. Guo,[1] Y. Guo,[1] Y. P. Guo,[22] Z. Haddadi,[25] A. Hafner,[22] S. Han,[51] X. Q. Hao,[15] F. A. Harris,[42] K. L. He,[1] T. Held,[4] Y. K. Heng,[1,a] Z. L. Hou,[1] C. Hu,[28] H. M. Hu,[1] J. F. Hu,[49a,49c] T. Hu,[1,a] Y. Hu,[1] G. S. Huang,[46,a] J. S. Huang,[15] X. T. Huang,[33] X. Z. Huang,[29] Y. Huang,[29] Z. L. Huang,[27] T. Hussain,[48] Q. Ji,[1] Q. P. Ji,[30] X. B. Ji,[1] X. L. Ji,[1,a] L. W. Jiang,[51] X. S. Jiang,[1,a] X. Y. Jiang,[30] J. B. Jiao,[33] Z. Jiao,[17] D. P. Jin,[1,a] S. Jin,[1] T. Johansson,[50] A. Julin,[43] N. Kalantar-Nayestanaki,[25] X. L. Kang,[1,*] X. S. Kang,[30] M. Kavatsyuk,[25] B. C. Ke,[5] P. Kiese,[22] R. Kliemt,[14] B. Kloss,[22] O. B. Kolcu,[40b,h] B. Kopf,[4] M. Kornicer,[42] A. Kupsc,[50] W. Kühn,[24] J. S. Lange,[24] M. Lara,[19] P. Larin,[14] C. Leng,[49c] C. Li,[50] Cheng Li,[46,a] D. M. Li,[53] F. Li,[1,a] F. Y. Li,[31] G. Li,[1] H. B. Li,[1] H. J. Li,[1] J. C. Li,[1] Jin Li,[32] K. Li,[33] K. Li,[13] Lei Li,[3] P. R. Li,[41] Q. Y. Li,[33] T. Li,[33] W. D. Li,[1] W. G. Li,[1] X. L. Li,[33] X. N. Li,[1,a] X. Q. Li,[30] Y. B. Li,[2] Z. B. Li,[38] H. Liang,[46,a] Y. F. Liang,[36] Y. T. Liang,[24] G. R. Liao,[11] D. X. Lin,[14] B. Liu,[34] B. J. Liu,[1] C. X. Liu,[1] D. Liu,[46,a] F. H. Liu,[35] Fang Liu,[1] Feng Liu,[6] H. B. Liu,[12] H. H. Liu,[16] H. H. Liu,[1] H. M. Liu,[1] J. Liu,[1] J. B. Liu,[46,a] J. P. Liu,[51] J. Y. Liu,[1] K. Liu,[39] K. Y. Liu,[27] L. D. Liu,[31] P. L. Liu,[1,a] Q. Liu,[41] S. B. Liu,[46,a] X. Liu,[26] Y. B. Liu,[30] Z. A. Liu,[1,a] Zhiqing Liu,[22] H. Loehner,[25] X. C. Lou,[1,b,h] H. J. Lu,[17] J. G. Lu,[1,a] Y. Lu,[1] Y. P. Lu,[1,a] C. L. Luo,[28] M. X. Luo,[52] T. Luo,[42] X. L. Luo,[1,a] X. R. Lyu,[41] F. C. Ma,[27] H. L. Ma,[1] L. L. Ma,[33] M. M. Ma,[1] Q. M. Ma,[1] T. Ma,[1] X. N. Ma,[30] X. Y. Ma,[1,a] Y. M. Ma,[33] F. E. Maas,[14] M. Maggiora,[49a,49c] Y. J. Mao,[31] Z. P. Mao,[1] S. Marcello,[49a,49c] J. G. Messchendorp,[25] J. Min,[1,a] T. J. Min,[1] R. E. Mitchell,[19] X. H. Mo,[1,a] Y. J. Mo,[6] C. Morales Morales,[14] N. Yu. Muchnoi,[9,e] H. Muramatsu,[43] Y. Nefedov,[23] F. Nerling,[14] I. B. Nikolaev,[9,e] Z. Ning,[1,a] S. Nisar,[8] S. L. Niu,[1,a] X. Y. Niu,[1] S. L. Olsen,[32] Q. Ouyang,[1,a] S. Pacetti,[20b] Y. Pan,[46,a] P. Patteri,[20a] M. Pelizaeus,[4] H. P. Peng,[46,a] K. Peters,[10,i] J. Pettersson,[50] J. L. Ping,[28] R. G. Ping,[1] R. Poling,[43] V. Prasad,[1] H. R. Qi,[2] M. Qi,[29] S. Qian,[1,a] C. F. Qiao,[41] L. Q. Qin,[33] N. Qin,[51] X. S. Qin,[1] Z. H. Qin,[1,a] J. F. Qiu,[1] K. H. Rashid,[48] C. F. Redmer,[22] M. Ripka,[22] G. Rong,[1] Ch. Rosner,[14] X. D. Ruan,[12] A. Sarantsev,[23,f] M. Savrié,[21b] K. Schoenning,[50] S. Schumann,[22] W. Shan,[31] M. Shao,[46,a] C. P. Shen,[2] P. X. Shen,[30] X. Y. Shen,[1] H. Y. Sheng,[1] M. Shi,[1] W. M. Song,[1] X. Y. Song,[1] S. Sosio,[49a,49c] S. Spataro,[49a,49c] G. X. Sun,[1] J. F. Sun,[15] S. S. Sun,[1] X. H. Sun,[1] Y. J. Sun,[46,a] Y. Z. Sun,[1] Z. J. Sun,[1,a] Z. T. Sun,[19] C. J. Tang,[36] X. Tang,[1] I. Tapan,[40c] E. H. Thorndike,[44] M. Tiemens,[25] M. Ullrich,[24] I. Uman,[40d] G. S. Varner,[42] B. Wang,[30] B. L. Wang,[41] D. Wang,[31] D. Y. Wang,[31] K. Wang,[1,a] L. L. Wang,[1] L. S. Wang,[1] M. Wang,[33] P. Wang,[1] P. L. Wang,[1] W. Wang,[1,a] W. P. Wang,[46,a] X. F. Wang,[39] Y. Wang,[37] Y. D. Wang,[14] Y. F. Wang,[1,a] Y. Q. Wang,[22] Z. Wang,[1,a] Z. G. Wang,[1,a] Z. H. Wang,[46,a] Z. Y. Wang,[1] Z. Y. Wang,[1] T. Weber,[22] D. H. Wei,[11] P. Weidenkaff,[22] S. P. Wen,[1] U. Wiedner,[4] M. Wolke,[50] L. H. Wu,[1] L. J. Wu,[1] Z. Wu,[1,a] L. Xia,[46,a] L. G. Xia,[39] Y. Xia,[18] D. Xiao,[1] H. Xiao,[47] Z. J. Xiao,[28] Y. G. Xie,[1,a] Q. L. Xiu,[1,a] G. F. Xu,[1] J. J. Xu,[1] L. Xu,[1] Q. J. Xu,[13] Q. N. Xu,[41] X. P. Xu,[37] L. Yan,[49a,49c] W. B. Yan,[46,a] W. C. Yan,[46,a] Y. H. Yan,[18] H. J. Yang,[34] H. X. Yang,[1] L. Yang,[51] Y. X. Yang,[11] M. Ye,[1,a] M. H. Ye,[7] J. H. Yin,[1] B. X. Yu,[1,a] C. X. Yu,[30] J. S. Yu,[26] C. Z. Yuan,[1] W. L. Yuan,[29] Y. Yuan,[1] A. Yuncu,[40b,b] A. A. Zafar,[48] A. Zallo,[20a] Y. Zeng,[18] Z. Zeng,[46,a] B. X. Zhang,[1] B. Y. Zhang,[1,a] C. Zhang,[29] C. C. Zhang,[1] D. H. Zhang,[1] H. H. Zhang,[38] H. Y. Zhang,[1,a] J. Zhang,[1] J. J. Zhang,[1] J. L. Zhang,[1] J. Q. Zhang,[1] J. W. Zhang,[1,a] J. Y. Zhang,[1] J. Z. Zhang,[1] K. Zhang,[1] L. Zhang,[1] S. Q. Zhang,[30] X. Y. Zhang,[33] Y. Zhang,[1] Y. H. Zhang,[1,a] Y. N. Zhang,[41] Y. T. Zhang,[46,a] Yu Zhang,[41] Z. H. Zhang,[6] Z. P. Zhang,[46] Z. Y. Zhang,[51] G. Zhao,[1] J. W. Zhao,[1,a] J. Y. Zhao,[1] J. Z. Zhao,[1,a] Lei Zhao,[46,a] Ling Zhao,[1] M. G. Zhao,[30] Q. Zhao,[1] Q. W. Zhao,[1] S. J. Zhao,[53] T. C. Zhao,[1] Y. B. Zhao,[1,a] Z. G. Zhao,[46,a] A. Zhemchugov,[23,c] B. Zheng,[47] J. P. Zheng,[1,a] W. J. Zheng,[33] Y. H. Zheng,[41] B. Zhong,[28] L. Zhou,[1,a] X. Zhou,[51] X. K. Zhou,[46,a] X. R. Zhou,[46,a] X. Y. Zhou,[1] K. Zhu,[1] K. J. Zhu,[1,a] S. Zhu,[1] S. H. Zhu,[45] X. L. Zhu,[39] Y. C. Zhu,[46,a] Y. S. Zhu,[1] Z. A. Zhu,[1] J. Zhuang,[1,a] L. Zotti,[49a,49c] B. S. Zou,[1] and J. H. Zou,[1]

(BESIII Collaboration)

[1]Institute of High Energy Physics, Beijing 100049, People's Republic of China
[2]Beihang University, Beijing 100191, People's Republic of China
[3]Beijing Institute of Petrochemical Technology, Beijing 102617, People's Republic of China
[4]Bochum Ruhr-University, D-44780 Bochum, Germany
[5]Carnegie Mellon University, Pittsburgh, Pennsylvania 15213, USA
[6]Central China Normal University, Wuhan 430079, People's Republic of China
[7]China Center of Advanced Science and Technology, Beijing 100190, People's Republic of China
[8]COMSATS Institute of Information Technology, Lahore, Defence Road, Off Raiwind Road, 54000 Lahore, Pakistan
[9]G.I. Budker Institute of Nuclear Physics SB RAS (BINP), Novosibirsk 630090, Russia
[10]GSI Helmholtzcentre for Heavy Ion Research GmbH, D-64291 Darmstadt, Germany
[11]Guangxi Normal University, Guilin 541004, People's Republic of China
[12]Guangxi University, Nanning 530004, People's Republic of China
[13]Hangzhou Normal University, Hangzhou 310036, People's Republic of China
[14]Helmholtz Institute Mainz, Johann-Joachim-Becher-Weg 45, D-55099 Mainz, Germany
[15]Henan Normal University, Xinxiang 453007, People's Republic of China
[16]Henan University of Science and Technology, Luoyang 471003, People's Republic of China
[17]Huangshan College, Huangshan 245000, People's Republic of China
[18]Hunan University, Changsha 410082, People's Republic of China
[19]Indiana University, Bloomington, Indiana 47405, USA
[20a]INFN Laboratori Nazionali di Frascati, I-00044 Frascati, Italy
[20b]INFN and University of Perugia, I-06100 Perugia, Italy
[21a]INFN Sezione di Ferrara, I-44122 Ferrara, Italy
[21b]University of Ferrara, I-44122 Ferrara, Italy
[22]Johannes Gutenberg University of Mainz, Johann-Joachim-Becher-Weg 45, D-55099 Mainz, Germany
[23]Joint Institute for Nuclear Research, 141980 Dubna, Moscow, Russia
[24]Justus-Liebig-Universitaet Giessen, II. Physikalisches Institut, Heinrich-Buff-Ring 16, D-35392 Giessen, Germany
[25]KVI-CART, University of Groningen, NL-9747 AA Groningen, The Netherlands
[26]Lanzhou University, Lanzhou 730000, People's Republic of China
[27]Liaoning University, Shenyang 110036, People's Republic of China
[28]Nanjing Normal University, Nanjing 210023, People's Republic of China
[29]Nanjing University, Nanjing 210093, People's Republic of China
[30]Nankai University, Tianjin 300071, People's Republic of China
[31]Peking University, Beijing 100871, People's Republic of China
[32]Seoul National University, Seoul 151-747, Korea
[33]Shandong University, Jinan 250100, People's Republic of China
[34]Shanghai Jiao Tong University, Shanghai 200240, People's Republic of China
[35]Shanxi University, Taiyuan 030006, People's Republic of China
[36]Sichuan University, Chengdu 610064, People's Republic of China
[37]Soochow University, Suzhou 215006, People's Republic of China
[38]Sun Yat-Sen University, Guangzhou 510275, People's Republic of China
[39]Tsinghua University, Beijing 100084, People's Republic of China
[40a]Ankara University, 06100 Tandogan, Ankara, Turkey
[40b]Istanbul Bilgi University, 34060 Eyup, Istanbul, Turkey
[40c]Uludag University, 16059 Bursa, Turkey
[40d]Near East University, Nicosia, North Cyprus, Mersin 10, Turkey
[41]University of Chinese Academy of Sciences, Beijing 100049, People's Republic of China
[42]University of Hawaii, Honolulu, Hawaii 96822, USA
[43]University of Minnesota, Minneapolis, Minnesota 55455, USA
[44]University of Rochester, Rochester, New York 14627, USA
[45]University of Science and Technology Liaoning, Anshan 114051, People's Republic of China
[46]University of Science and Technology of China, Hefei 230026, People's Republic of China
[47]University of South China, Hengyang 421001, People's Republic of China
[48]University of the Punjab, Lahore-54590, Pakistan
[49a]University of Turin, I-10125 Turin, Italy
[49b]University of Eastern Piedmont, I-15121 Alessandria, Italy
[49c]INFN, I-10125 Turin, Italy
[50]Uppsala University, Box 516, SE-75120 Uppsala, Sweden
[51]Wuhan University, Wuhan 430072, People's Republic of China

^{52}*Zhejiang University, Hangzhou 310027, People's Republic of China*
^{53}*Zhengzhou University, Zhengzhou 450001, People's Republic of China*

Based on a sample of 1.31×10^9 J/ψ events collected with the BESIII detector, an amplitude analysis of the isospin-violating decays $\eta' \to \pi^+\pi^-\pi^0$ and $\eta' \to \pi^0\pi^0\pi^0$ is performed. A significant P-wave contribution from $\eta' \to \rho^\pm\pi^\mp$ is observed for the first time in $\eta' \to \pi^+\pi^-\pi^0$. The branching fraction is determined to be $\mathcal{B}(\eta' \to \rho^\pm\pi^\mp) = (7.44 \pm 0.60 \pm 1.26 \pm 1.84) \times 10^{-4}$, where the first uncertainty is statistical, the second systematic, and the third model dependent. In addition to the nonresonant S-wave component, there is a significant σ meson component. The branching fractions of the combined S-wave components are determined to be $\mathcal{B}(\eta' \to \pi^+\pi^-\pi^0)_S = (37.63 \pm 0.77 \pm 2.22 \pm 4.48) \times 10^{-4}$ and $\mathcal{B}(\eta' \to \pi^0\pi^0\pi^0) = (35.22 \pm 0.82 \pm 2.54) \times 10^{-4}$, respectively. The latter one is consistent with previous BESIII measurements.

The decays $\eta' \to \pi\pi\pi$ are isospin-violating processes. Because the electromagnetic contribution is strongly suppressed [1,2], they are induced dominantly by the strong interaction via the explicit breaking of chiral symmetry by the $d - u$ quark mass difference. In recent years, there has been considerable interest in these decays because they allow the determination of the light quark mass difference using the ratios of decay widths, $r_\pm = \mathcal{B}(\eta' \to \pi^+\pi^-\pi^0)/\mathcal{B}(\eta' \to \pi^+\pi^-\eta)$ and $r_0 = \mathcal{B}(\eta' \to \pi^0\pi^0\pi^0)/\mathcal{B}(\eta' \to \pi^0\pi^0\eta)$ [3,4]. Within the framework of chiral effective field theory combined with a relativistic coupled-channel approach, Ref. [5] predicts that the $\eta' \to \rho^\pm\pi^\mp$ P-wave contribution should be large for $\eta' \to \pi^+\pi^-\pi^0$. For the channel with three neutral pions, $\eta' \to \pi^0\pi^0\pi^0$, the P-wave contribution in two-body rescattering is forbidden by Bose symmetry. In general, the final-state interaction is expected to be very important because it was already found to be essential to explain the decay width of $\eta \to \pi\pi\pi$ [6,7]. In the case of η' decays, the final-state interaction is further enhanced due to the presence of nearby resonances and is expected to strongly affect the values of the branching fractions and the Dalitz plot distributions.

So far, there is no direct experimental evidence of an intermediate $\rho^\pm$ contribution to the decay $\eta' \to \pi^+\pi^-\pi^0$. In 2009, the CLEO-c experiment [8] reported the first observation of $\eta' \to \pi^+\pi^-\pi^0$ with $20.2^{+6.1}_{-4.8}$ events, corresponding to a branching fraction of $(37 \pm 11) \times 10^{-4}$, and a Dalitz plot consistent with a flat distribution. Recently the decay was also observed by the BESIII experiment [9] with a branching fraction consistent with the CLEO-c result; however, no Dalitz plot analysis was presented. Interest in the decay channel $\eta' \to \pi^0\pi^0\pi^0$ stems from the observed 4σ discrepancy between the recent branching fraction measurement by BESIII [$(35.6 \pm 4.0) \times 10^{-4}$] [9] and those from all previous experiments [10–12]. The BESIII result indicates a value for the ratio r_0 that is two times larger than previous experiments. Furthermore, the recent determination of the Dalitz plot slope parameter for $\eta' \to \pi^0\pi^0\pi^0$ decay gave $\alpha = -0.687 \pm 0.061$ [13],

which deviates significantly from that for the phase-space distribution ($\alpha = 0$). This implies that final-state interactions play an essential role. In this Letter, we present an amplitude analysis combining $\eta' \to \pi^+\pi^-\pi^0$ and $\eta' \to \pi^0\pi^0\pi^0$ events originating from J/ψ radiative decays using 1.31×10^9 J/ψ events [14,15] accumulated by the BESIII detector, which is described in detail in Ref. [16].

For a $J/\psi \to \gamma\eta'$ with $\eta' \to \pi^+\pi^-\pi^0$ candidate event, two tracks with opposite charge and at least three photon candidates are required. The selection criteria for charged tracks and photon candidates are the same as those in Ref. [13]. Because the radiative photon from the J/ψ is always more energetic than the photons from the π^0 decays, the photon candidate with the maximum energy in the event is taken as the radiative one. For each $\pi^+\pi^-\gamma\gamma\gamma$ combination, a six-constraint (6C) kinematic fit is performed, and the χ^2_{6C} is required to be less than 25. The fit enforces energy-momentum conservation and constrains the invariant masses of the other photon pair and $\pi^+\pi^-\pi^0$ to the nominal π^0 and η' mass, respectively. If there are more than three photon candidates in an event, the combination with the smallest χ^2_{6C} is retained. To reject possible backgrounds with two or four photons in the final states, we further require that the probability of the 4C kinematic fit imposing energy-momentum conservation for the $J/\psi \to \pi^+\pi^-\gamma\gamma\gamma$ signal hypothesis is larger than that for the $J/\psi \to \pi^+\pi^-\gamma\gamma$ and $J/\psi \to \pi^+\pi^-\gamma\gamma\gamma\gamma$ background hypotheses. Additionally, events with $|M(\gamma\pi^0) - m_\omega| < 0.05$ GeV/c^2 are rejected to suppress background from $J/\psi \to \omega\pi^+\pi^-$.

With the above requirements, a sample of 8267 events is selected, and the corresponding Dalitz plot is shown in Fig. 1(a), where two clusters of events corresponding to the decays of $\eta' \to \rho^\pm\pi^\mp$ are observed. The possible background events are investigated with a Monte Carlo (MC) sample of $1.2 \times 10^9 J/\psi$ inclusive decays generated with the LUNDCHARM and EVTGEN models [17,18]. Using the same selection criteria, the surviving background events mainly originate from the decay $\eta' \to \gamma\rho$ with $\rho \to \pi\pi$ or $\rho \to \gamma\pi\pi$, which accumulate in a peak around the η' mass
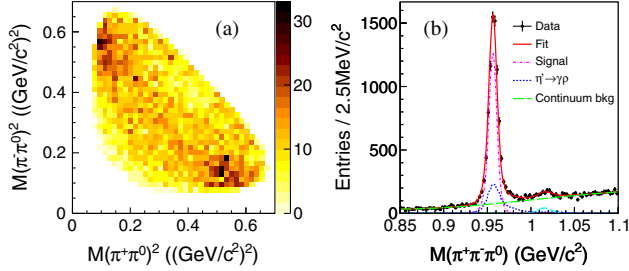
FIG. 1. (a) $\eta' \to \pi^+\pi^-\pi^0$ Dalitz plot for candidate events selected from data. (b) Invariant mass distribution of $\pi^+\pi^-\pi^0$ candidates without the η' mass constraint applied in the kinematic fit.

region, and the nonpeaking processes with multiphotons in the final states, e.g., $J/\psi \to \pi^+\pi^-\pi^0\pi^0$. However, none of these backgrounds contribute to the clusters around the $\rho^{\pm}$ mass region. For $\eta' \to \gamma\rho$, a study with a dedicated MC simulation based on an amplitude analysis of the same BESIII data and Ref. [19] and using the branching fractions of $J/\psi \to \gamma\eta'$ and $\eta' \to \gamma\rho$, $\rho \to \pi\pi/\gamma\pi\pi$, $\pi^0 \to \gamma\gamma$ [20] predicts the number of events from this background to be 1362 ± 54.

The decay $J/\psi \to \pi^+\pi^-\pi^0\pi^0$, which is assumed to represent the nonpeaking background contribution, is not well known. In order to estimate this background, an alternative data sample is selected by using a 5C kinematic fit without the η' mass constraint. The resulting $\pi^+\pi^-\pi^0$ invariant mass spectrum is shown in Fig. 1(b), where the η' peak is clearly visible. We then perform an unbinned maximum likelihood fit to the $M(\pi^+\pi^-\pi^0)$ distribution where the signal is described by the MC simulated shape convolved with a Gaussian resolution function, the peaking background ($\eta' \to \gamma\rho$) is described by the MC simulated shape, and the nonpeaking background contribution by a second-order Chebyshev polynomial function. The number of $\eta' \to \gamma\rho$ events is fixed to the expected value, while the small peak around 1.02 GeV/c^2 from $J/\psi \to \gamma\gamma\phi$ events is described with a Gaussian function. The number of non-peaking background events in the selected 6C-fitted sample is estimated to be 838 ± 31, using the number of background events from the 5C-fitted sample in the η' signal region ($|M(\pi^+\pi^-\pi^0) - 0.958| < 0.02$ GeV/c^2) and taking into account the slight difference of detection efficiency between 5C and 6C kinematic requirements. To further verify the above background estimation, we checked the background shapes in $\pi\pi$ mass spectra of the data. For each mass bin, the number of background events is extracted by fitting the $\pi^+\pi^-\pi^0$ mass spectrum in this bin. We found that the background shapes are consistent with those estimated from the MC simulations. (More details are given in the Supplemental Material [21]).

For $J/\psi \to \gamma\eta'$ with $\eta' \to \pi^0\pi^0\pi^0$, events containing at least seven photon candidates and no charged tracks are selected. The photon selection criteria are the same as those

for $\eta' \to \pi^+\pi^-\pi^0$. The photon with the maximum energy in the event is assumed to be the radiative photon originating from the decay of J/ψ. For the remaining photon candidates, pairs of photons are combined to form $\pi^0 \to \gamma\gamma$ candidates which are subjected to a 1C kinematic fit, where the invariant mass of the photon pair is constrained to the nominal π^0 mass, and the χ^2 value is required to be less than 25. To suppress π^0 miscombinations, the π^0 decay angle (θ_{decay}), defined as the polar angle of a photon in the corresponding $\gamma\gamma$ rest frame, is required to satisfy $|\cos\theta_{\text{decay}}| < 0.95$. From the accepted π^0 candidates and the corresponding radiative photon, $\gamma\pi^0\pi^0\pi^0$ combinations are formed. A kinematic fit with eight constraints (8C) is performed, constraining the invariant masses of $\gamma\gamma$ pairs and $\pi^0\pi^0\pi^0$ candidates to the nominal π^0 and η' masses, respectively. Events with $\chi^2_{8C} < 70$ are accepted for further analysis. If there is more than one combination, only the one with the smallest χ^2_{8C} is retained. To suppress possible background from $J/\psi \to \gamma\eta\pi^0\pi^0$, a 7C kinematic fit is performed under the $J/\psi \to \gamma\eta\pi^0\pi^0$ hypothesis and events for which the probability of this 7C fit is larger than that of the signal hypothesis are discarded. In addition, events which have at least one $\gamma\gamma$ pair with invariant mass within the η signal region, $(0.52, 0.59)$ GeV/c^2, are rejected. Possible background from $J/\psi \to \omega\pi^0\pi^0$ is suppressed by vetoing events with $|M(\gamma\pi^0) - m_{\omega}| < 0.05$ GeV/c^2, where $M(\gamma\pi^0)$ is the invariant mass of a $\gamma\pi^0$ combination.

The three π^0 candidates selected are ordered as π_1^0, π_2^0, and π_3^0, according to their descending energies in the η' rest frame, and the corresponding Dalitz plot is displayed in Fig. 2(a) for the 2237 events selected. The analysis of the inclusive MC sample of 1.2×10^9 J/ψ decays indicates a low background level, including the peaking background originating from $J/\psi \to \gamma\eta'$ with $\eta' \to \eta\pi^0\pi^0$ and the nonpeaking background mainly coming from $J/\psi \to \gamma\pi^0\pi^0\pi^0$, since the decay of $J/\psi \to \pi^0\pi^0\pi^0\pi^0$ is forbidden. The number of background events from $\eta' \to \eta\pi^0\pi^0$ is estimated to be 46 ± 3, using a MC sample with the decay amplitudes from Ref. [22]. Similarly, we perform a 7C kinematic fit without applying the constraint on the η' mass to estimate the nonpeaking background. The fit to the $M(\pi^0\pi^0\pi^0)$ distribution is displayed in Fig. 2(b) using the simulated shape convolved with a Gaussian resolution function for the signal, a MC simulated peaking background shape, and a second-order polynomial function for non-peaking background events. The number of the nonpeaking background events in the selected $\eta' \to \pi^0\pi^0\pi^0$ sample, predominantly originating from $J/\psi \to \gamma\pi^0\pi^0\pi^0$, is estimated to be 176 ± 24 after taking into account the detection efficiencies with and without the η' mass constraint.

A Dalitz plot analysis based on the formalism of the isobar model [23] is performed. The resonant π-π S-wave ($L = 0$ for σ) and P-wave ($L = 1$ for $\rho^{\pm}$) amplitudes are described following the formalism from Ref. [24],
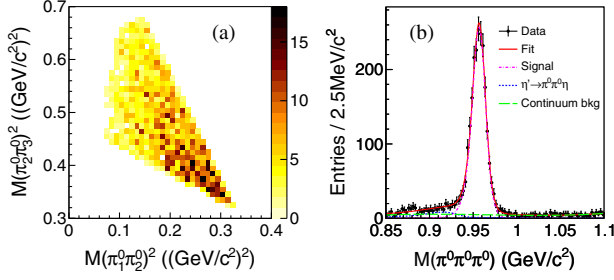
FIG. 2. (a) $\eta' \to \pi^0\pi^0\pi^0$ Dalitz plot for candidate events selected from data. (b) Invariant mass of $\pi^0\pi^0\pi^0$ candidates without the η' mass constraint applied in the kinematic fit.

$$W(s) = \frac{1}{\cot\delta_L(s) - i}, \tag{1}$$

where

$$\cot\delta_0(s) = \frac{\sqrt{s}}{2k}\frac{M_\pi^2}{s - M_\pi^2/2}\left(\frac{M_\pi}{\sqrt{s}} + B_0^S + B_1^S\omega_0(s)\right),$$

$$\cot\delta_1(s) = \frac{\sqrt{s}}{2k^3}(M_\rho^2 - s)\left(\frac{2M_\pi^3}{M_\rho^2\sqrt{s}} + B_0^P + B_1^P\omega_1(s)\right),$$

$$\omega_L(s) = \frac{\sqrt{s} - \sqrt{s_L - s}}{\sqrt{s} + \sqrt{s_L - s}} - 1.$$

Here s is the $\pi\pi$ invariant mass square, $k = \sqrt{s/4 - M_\pi^2}$, $\sqrt{s_0} = 2M_K$, the masses M_ρ, M_K, and M_π are fixed to the world average values [20], $\sqrt{s_1} = 1.05$ GeV is a constant, and B_0^S, B_1^S, B_0^P, and B_1^P are free parameters.

The free parameters of the probability density function (PDF) are optimized with an unbinned maximum likelihood fit using both the $\eta' \to \pi^+\pi^-\pi^0$ and $\eta' \to \pi^0\pi^0\pi^0$ events, where the background contributions are included as noninterfering terms in the PDF and are fixed according to the MC simulation, the mass resolution, and the detection efficiency obtained from the MC simulation are taken into account in the signal PDF. The fit minimizes the negative log-likelihood value $-\ln\mathcal{L} = -\sum_{i=1}^{N_1}\ln\mathcal{P}_i - \sum_{j=1}^{N_2}\ln\mathcal{P}'_j$, where $\mathcal{P}_i$ and $\mathcal{P}'_j$ are the PDFs for an $\eta' \to \pi^+\pi^-\pi^0$ event i and an $\eta' \to \pi^0\pi^0\pi^0$ event j, respectively. The sum runs over all accepted events. From charge conjugation invariance, the magnitude and phase for ρ^+ and ρ^- are taken to be the same in the nominal fit.

Projections of the data and fit results are displayed in Fig. 3. The data are well described by three components: P wave ($\rho^\pm\pi^\mp$), resonant S wave ($\sigma\pi^0$), and phase-space S wave ($\pi\pi\pi$). The interference between σ and the nonresonant term is large and strongly depends on the parametrization of σ. Therefore we are unable to determine the individual contributions and consider only the sum of the S-wave amplitudes in this analysis. To estimate the significance of each component, the fit is repeated with the corresponding amplitude excluded and the statistical
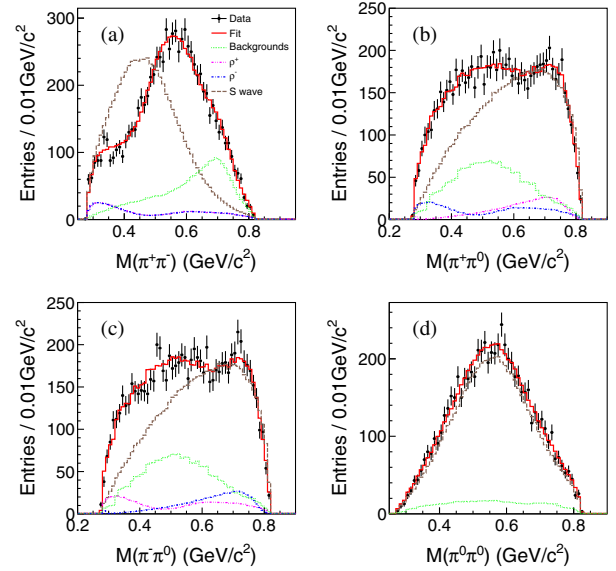

FIG. 3. Comparison of the invariant mass distributions of (a) $\pi^+\pi^-$, (b) $\pi^+\pi^0$, (c) $\pi^-\pi^0$, and (d) $\pi^0\pi^0$ between data (dots with error bars) and the fit result projections (solid histograms). The dotted, dashed, dash-dotted, and dash-dot-dotted histograms show the contributions from background, S wave, ρ^-, and ρ^+, respectively.

significance is then determined by the changes of the $-2\ln\mathcal{L}$ value, with the number of degrees of freedom equal to twice the number of extra parameters in the fit [25]. The statistical significances of all three components are found to be larger than 24σ. To check for an additional contribution, we add an amplitude for the scalar meson $f_0(980)$, described by the Flatté function [26] with the parameters fixed using values from Ref. [27]. The corresponding statistical significance is only 0.3σ, and the contribution is therefore neglected.

With the fitted values of $B_0^P = 2.685 \pm 0.006$, $B_1^P = 1.740 \pm 0.004$, $B_0^S = -39.09 \pm 5.66$, and $B_1^S = -39.18 \pm 4.64$, the corresponding poles of ρ and σ are determined to be $775.49(\text{fixed}) - i(68.5 \pm 0.2)$ MeV and $(512 \pm 15) - i(188 \pm 12)$ MeV, respectively, and are therefore in reasonable agreement with the $\rho^\pm$ and σ values from the Particle Data Group (PDG) [20]. The signal yields defined as the integrals over the Dalitz plot of a single decay amplitude squared, the detection efficiencies obtained from the MC sample weighted with each amplitude, and the branching fractions for each component are summarized in Table I. In the calculation, the number of J/ψ is taken from Refs. [14,15], and the branching fraction for $J/\psi \to \gamma\eta'$ and $\pi^0 \to \gamma\gamma$ are taken from the PDG [20].

In order to compare with previous measurements, which did not consider the P-wave contribution [8,9], we also provide the branching fraction of $\eta' \to \pi^+\pi^-\pi^0$ calculated with the total number of observed signal events, which is presented in Table I.

TABLE I. Yields with statistical errors, detection efficiencies, and branching fractions for the studied η' decay modes, where the first errors are statistical, the second systematic, and the third model dependent.

Decay mode	Yield	ε (%)	$\mathcal{B}$ (10^{-4})
$\pi^+\pi^-\pi^0$	6067 ± 91	25.3	$35.91 \pm 0.54 \pm 1.74$
$\pi^0\pi^0\pi^0$	2015 ± 47	8.8	$35.22 \pm 0.82 \pm 2.54$
$\rho^\pm\pi^\mp$	1231 ± 98	24.8	$7.44 \pm 0.60 \pm 1.26 \pm 1.84$
$(\pi^+\pi^-\pi^0)_S$	6580 ± 134	26.2	$37.63 \pm 0.77 \pm 2.22 \pm 4.48$

To check charge conjugation in the P-wave process, alternative fits were performed with different magnitudes and phases for ρ^+ and ρ^-. The result is consistent with charge symmetry, $[\mathcal{B}(\eta' \to \rho^+\pi^-) - \mathcal{B}(\eta' \to \rho^-\pi^+)]/[\mathcal{B}(\eta' \to \rho^+\pi^-) + \mathcal{B}(\eta' \to \rho^-\pi^+)] = 0.053 \pm 0.060\text{(stat)} \pm 0.010\text{(syst)}$.

As an alternative model, the Gounaris-Sakurai parametrization [28] is used to describe the $\rho^\pm$ contribution with the mass and width fixed to the PDG values [20]. The $-\ln \mathcal{L}$ value is only worse by 0.9. In another check the $\pi-\pi$ S wave for σ is replaced with a relativistic Breit-Wigner function. This fit also provides a reasonable description of the data, and the $-\ln \mathcal{L}$ value only changes by 3.5. The mass and width determined from this fit are (538 ± 12) MeV/c^2 and (363 ± 20) MeV, respectively, which are compatible with the pole position of the $\pi-\pi$ elastic scattering amplitude.

Based on the symmetry imposed by Bose-Einstein statistics and isospin [29,30], the magnitude of the non-resonant S-wave amplitude in $\eta' \to \pi^0\pi^0\pi^0$ is three times that in $\eta' \to \pi^+\pi^-\pi^0$. If this constraint is introduced, the fitted yields are compatible with the unconstrained result, while the change in $-\ln \mathcal{L}$ is 8.4, corresponding to a statistical significance of 3.7σ.

The differences of the branching fractions for the above tests contribute to the systematic uncertainties, denoted as model and constraint in Table II, respectively. In addition,

TABLE II. Summary of systematic uncertainties for the determination of branching fractions for each component.

Source	$\rho^\pm\pi^\mp$ (%)	$(\pi^+\pi^-\pi^0)_S$ (%)	$\pi^+\pi^-\pi^0$ (%)	$\pi^0\pi^0\pi^0$ (%)
Constraint	15.9	3.3	$\cdots$	$\cdots$
MDC tracking	2	2	2	$\cdots$
Radiative photon	1	1	1	1
π^0 selection	2	2	2	6
Kinematic fit	1.7	1.7	1.7	1.6
Background	3.0	1.4	1.2	1.3
Number of J/ψ	0.8	0.8	0.8	0.8
$\mathcal{B}(J/\psi \to \gamma\eta')$	3.1	3.1	3.1	3.1
Total	16.9	5.9	4.9	7.2
Model	24.7	11.9	$\cdots$	$\cdots$

the following sources of the systematic uncertainty are considered: The uncertainties in main drift chamber (MDC) tracking, photon selection and π^0 reconstruction efficiency (including photon detection efficiency) are studied using a high purity control sample of $J/\psi \to \rho\pi$. The differences between data and MC simulation are less than 1% per charged track, 1% for the radiative photon and 2% per π^0. The uncertainties associated with kinematic fits are studied using the control sample $J/\psi \to \gamma\eta \to \gamma\pi\pi\pi$. The preliminary selection conditions for good charged tracks, good photons, and π^0 candidates are the same as those for $J/\psi \to \gamma\eta' \to \gamma\pi\pi\pi$. The differences between data and MC simulation for the requirements of $\chi^2_{6C}(\gamma\pi^+\pi^-\pi^0) < 25$ and $\chi^2_{8C}(\gamma\pi^0\pi^0\pi^0) < 70$ are determined as 1.7% and 1.6%, respectively.

To investigate the uncertainties of the background determination, alternative fits are performed on the background components one at a time. The peaking backgrounds $\eta' \to \gamma\rho$ and $\eta' \to \pi^0\pi^0\eta$ are varied according to the errors of the branching fraction for $J/\psi \to \gamma\eta'$ and the cascade decays in the PDG [20]. The continuum background is varied according to the uncertainties of the fits to the $\pi\pi$ mass spectra. Different selection criteria for vetoing ω background are also used. The differences of the branching fractions with respect to the default values are taken as the uncertainties associated with backgrounds.

All the systematic uncertainties including the uncertainty from the number of J/ψ events and the branching fraction of $J/\psi \to \gamma\eta'$ are summarized in Table II, where the total systematic uncertainty is given by the quadratic sum, assuming all sources to be independent.

In summary, using a combined amplitude analysis of $\eta' \to \pi^+\pi^-\pi^0$ and $\eta' \to \pi^0\pi^0\pi^0$ decays, the P-wave contribution from $\rho^\pm$ is observed for the first time with high statistical significance. The pole position of $\rho^\pm$, $775.49\text{(fixed)} - i(68.5 \pm 0.2)$ MeV, is consistent with previous measurements, and the branching fraction $\mathcal{B}(\eta' \to \rho^\pm\pi^\mp)$ is determined to be $(7.44 \pm 0.60 \pm 1.26 \pm 1.84) \times 10^{-4}$.

In addition to the nonresonant S wave, the resonant $\pi-\pi S$ wave with a pole at $(512 \pm 15) - i(188 \pm 12)$ MeV, interpreted as the broad σ meson, plays an essential role in the $\eta' \to \pi\pi\pi$ decays. Because of the large interference between nonresonant and resonant S waves, only the

sum is used to describe the S-wave contribution, and the branching fractions are determined to be $\mathcal{B}(\eta' \to \pi^+\pi^-\pi^0)_S = (37.63 \pm 0.77 \pm 2.22 \pm 4.48) \times 10^{-4}$ and $\mathcal{B}(\eta' \to \pi^0\pi^0\pi^0) = (35.22 \pm 0.82 \pm 2.54) \times 10^{-4}$, respectively. The branching fractions of $\eta' \to \pi^+\pi^-\pi^0$ and $\eta' \to \pi^0\pi^0\pi^0$ are in good agreement with and supersede the previous BESIII measurements [9]. The value for $\mathcal{B}(\eta' \to \pi^0\pi^0\pi^0)$ is two times larger than that from GAMS $[(16.0 \pm 3.2) \times 10^{-4}]$ [11]. The significant resonant S-wave contribution also provides a reasonable explanation for the negative slope parameter of the $\eta' \to \pi^0\pi^0\pi^0$ Dalitz plot [13]. The ratio of the branching fractions between the S-wave components $\mathcal{B}(\eta' \to \pi^0\pi^0\pi^0)/\mathcal{B}(\eta' \to \pi^+\pi^-\pi^0)_S$ is determined to be $0.94 \pm 0.03 \pm 0.13$, where the common systematic uncertainties cancel out. With the branching fractions of $\eta' \to \pi\pi\eta$ taken from the PDG [20], $r_{\pm}$ and r_0 are now calculated to be $(8.77 \pm 1.19) \times 10^{-3}$ and $(15.86 \pm 1.33) \times 10^{-3}$, respectively. While the previous values based on the PDG [20] are $(8.86 \pm 0.94) \times 10^{-3}$ and $(9.64 \pm 0.97) \times 10^{-3}$, respectively.

The observed substantial P- and S-wave resonant contributions have to be properly considered by theory before attempting to determine light quark masses from $r_{\pm}$ and r_0. In particular, one of the previously most comprehensive analyses of hadronic decays of η and η' mesons relied on r_0, which is now two times larger, and $r_{\pm}$ was not known [4]. Further progress will depend on the development of dispersive approaches such as Refs. [31–34] for η' hadronic decays.

*Corresponding author.
kangxl@ihep.ac.cn
[a]Also at State Key Laboratory of Particle Detection and Electronics, Beijing 100049, Hefei 230026, People's Republic of China.
[b]Also at Bogazici University, 34342 Istanbul, Turkey.
[c]Also at Moscow Institute of Physics and Technology, Moscow 141700, Russia.
[d]Also at Functional Electronics Laboratory, Tomsk State University, Tomsk 634050, Russia.
[e]Also at Novosibirsk State University, Novosibirsk 630090, Russia.
[f]Also at NRC Kurchatov Institute, PNPI, 188300 Gatchina, Russia.
[g]Also at University of Texas at Dallas, Richardson, Texas 75083, USA.
[h]Also at Istanbul Arel University, 34295 Istanbul, Turkey.
[i]Also at Goethe University Frankfurt, 60323 Frankfurt am Main, Germany.

[1] D. G. Sutherland, Phys. Lett. **23**, 384 (1966).
[2] R. Baur, J. Kambor, and D. Wyler, Nucl. Phys. **B460**, 127 (1996).
[3] D. J. Gross, S. B. Treiman, and F. Wilczek, Phys. Rev. D **19**, 2188 (1979).
[4] B. Borasoy, U.-G. Meißner, and R. Nißler, Phys. Lett. B **643**, 41 (2006).
[5] B. Borasoy and R. Nißler, Eur. Phys. J. A **26**, 383 (2005).
[6] J. Gasser and H. Leutwyler, Nucl. Phys. **B250**, 539 (1985).
[7] J. Bijnens and K. Ghorbani, J. High Energy Phys. 11 (2007) 030.
[8] P. Naik et al. (CLEO Collaboration), Phys. Rev. Lett. **102**, 061801 (2009).
[9] M. Ablikim et al. (BESIII Collaboration), Phys. Rev. Lett. **108**, 182001 (2012).
[10] F. G. Binon et al., Phys. Lett. **140B**, 264 (1984).
[11] D. Alde, F. G. Binon, and C. Bricman, Z. Phys. C **36**, 603 (1987).
[12] A. M. Blik et al. (GAMS-4π Collaboration), Phys. At. Nucl. **71**, 2124 (2008).
[13] M. Ablikim et al. (BESIII Collaboration), Phys. Rev. D **92**, 012014 (2015).
[14] M. Ablikim et al. (BESIII Collaboration), Chin. Phys. C **36**, 915 (2012).
[15] With the same approach as for J/ψ events taken in 2009 (see Ref. [14] for more details), the preliminary number of J/ψ events taken in 2009 and 2012 is determined to be 1310.6×10^6 with an uncertainty of 0.8%.
[16] M. Ablikim et al. (BESIII Collaboration), Nucl. Instrum. Methods Phys. Res., Sect. A **614**, 345 (2010).
[17] J. C. Chen, G. S. Huang, X. R. Qi, D. H. Zhang, and Y. S. Zhu, Phys. Rev. D **62**, 034003 (2000).
[18] D. J. Lange, Nucl. Instrum. Methods Phys. Res., Sect. A **462**, 152 (2001).

[19] G. Toledo Sánchez, J. L. García-Luna, and V. González-Enciso, Phys. Rev. D **76**, 033001 (2007).

[20] K. A. Olive *et al.* (Particle Data Group), Chin. Phys. C **38**, 090001 (2014).

[21] See Supplemental Material at http://link.aps.org/supplemental/10.1103/PhysRevLett.118.012001 for additional information on the verification of the background estimation.

[22] A. M. Blik *et al.* (GAMS-4π Collaboration), Phys. At. Nucl. **72**, 231 (2009).

[23] M. Ablikim *et al.* (BESIII Collaboration), Phys. Rev. D **89**, 052001 (2014).

[24] R. García-Martín, R. Kamiński, J. R. Peláez, J. Ruiz de Elvira, and F. J. Ynduráin, Phys. Rev. D **83**, 074004 (2011).

[25] R. Aaij *et al.* (LHCb Collaboration), Phys. Rev. Lett. **115**, 072001 (2015).

[26] S. M. Flatté, Phys. Lett. **63B**, 224 (1976).

[27] M. Ablikim *et al.* (BESIII Collaboration), Phys. Lett. B **607**, 243 (2005).

[28] G. J. Gounaris and J. J. Sakurai, Phys. Rev. Lett. **21**, 244 (1968).

[29] C. Zemach, Phys. Rev. **133**, B1201 (1964).

[30] J. Bijnens and J. Gasser, Phys. Scr. **T99**, 34 (2002).

[31] G. Colangelo, S. Lanz, and E. Passemar, Proc. Sci., CD09 (**2009**) 047.

[32] S. P. Schneider, B. Kubis, and C. Ditsche, J. High Energy Phys. 02 (2011) 028.

[33] K. Kampf, M. Knecht, J. Novotny, and M. Zdrahal, Phys. Rev. D **84**, 114015 (2011).

[34] P. Guo, I. V. Danilkin, D. Schott, C. Fernández-Ramírez, V. Mathieu, and A. P. Szczepaniak, Phys. Rev. D **92**, 054016 (2015).